Journal of Solid State Chemistry 182 (2009) 1149–1155

Contents lists available at ScienceDirect

Journal of Solid State Chemistry

journal homepage: www.elsevier.com/locate/jssc

Template-free polyoxometalate-assisted synthesis for ZnO hollow spheres

Qiuyu Li [a,b], Enbo Wang [a,*], Siheng Li [a], Chunlei Wang [a], Chungui Tian [a], Guoying Sun [a], Jianmin Gu [a], Rui Xu [a]

[a] Key Laboratory of Polyoxometalate Science of Ministry of Education, Department of Chemistry, Northeast Normal University, Ren Min Street No. 5268, Changchun, Jilin 130024, PR China

[b] Department of Bioengineering, Jilin Business and Technology College, Xi An Road No. 4728, Changchun, Jilin 130062, PR China

ARTICLE INFO

Article history:
Received 25 June 2008
Received in revised form
23 October 2008
Accepted 26 October 2008
Available online 20 November 2008

Keywords:
ZnO
Hollow spheres
Polyoxometalate
Photoluminescence properties

ABSTRACT

ZnO hollow spheres with diameters ranging from 400 to 600 nm and the thickness of shell approximate 80 nm were synthesized by a simple polyoxometalate-assisted solvothermal route without using any templates. The effect of polyoxometalate concentration, reaction time and temperature on the formation of the hollow spheres was investigated. The results indicated that the hollow spheres were composed of porous shells with nanoparticles and polyoxometalate play a key role in controlling morphology of ZnO. A possible growth mechanism based on polyoxometalate-assisted assembly and slow Ostwald ripening dissolution in ethanol solution is tentatively proposed. In addition, the room temperature photoluminescence spectrum showed that the ZnO hollow spheres exhibit exciting emission features with wide band covering nearly all the visible region.

1. Introduction

Hollow structures of nanomaterials have recently attracted increasing attention owing to their wide applications in catalysis, controlled delivery, artificial cells, light fillers, low dielectric constant materials, acoustic insulation, and photonic crystals [1–4]. Zinc oxide, an important semiconductor with a direct band gap (3.37 eV) and a relatively high exciton binding energy (60 meV), has attracted more and more interest in tailoring its desired shape due to various shape-induced functions. Recently, great interest has focused on synthesis of ZnO hollow spheres duo to their potential applications in the delivery of drugs, catalysis, chemical storage, microcapsule reactors, photoelectric materials and so on [3,5–8]. One general approach for preparing ZnO hollow spheres is template technology based on various organic or inorganic templates including polystyrene [9,10], carbon spheres [11] and spherobacteria [12], which has been proven to be an effective route for synthesis of ZnO hollow spheres. However, introduction of impurities to the products is usually inevitable and the removal of the templates requires additional processing steps that can be costly, wasteful and of environmental concern. In contrast, the template-free preparative strategy concerning physical phenomena such as the "Kirkendall effect" or "Ostwald ripening" is a more simple and effective alternative, aiming at a "one-pot" self-assembly for ZnO hollow spheres. Recently, ZnO hollow dandelion-like spheres were synthesized through a Kirkendall effect under hydrothermal conditions [13]. Organic polymer-assisted and surfactant-assisted hydrothermal methods were employed to synthesize ZnO hollow spheres by Ostwald ripening process [14–16]. Therefore, it is rationally desired to explore simple template-free methods for the preparation of ZnO hollow spheres meeting the need of future large-scale production and applications.

Polyoxometalates (POMs) are a class of inorganic metal-oxygen cluster compounds with unique molecular structure, electronic versatility and chemical characters [17]. Recently, POMs were also introduced into the morphology-controlled synthesis of nano/microstructures [18–20]. Kuhn's group adsorbed POMs on carbon surfaces to obtain highly dispersed colloidal carbon with quite a narrow size distribution [19]. POMs have been used to stabilize platinum nanoparticles based on their physical presence and electrostatic properties [20]. Silicon quantum dots were successfully synthesized by POM-assisted electrochemical deposition [21]. Our group has also reported the POM-assisted growth of carbon nanotube, hematite hollow microspheres and iron oxide nanorods [22–24].

In this paper, a facile template-free solvothermal route is developed for rational fabrication of ZnO hollow spheres by the forced alcoholysis process of zinc acetate in presence of tungstophosphoric acid ($H_3PW_{12}O_{40}$: HPW), a kind of Keggin-type POMs. Series of experiments showed that HPW played a key role in the formation of ZnO hollow spheres. A possible growth mechanism of the as-prepared ZnO hollow spheres was proposed.

* Corresponding author. Fax: +86 431 85098787.
E-mail addresses: wangeb889@nenu.edu.cn, wangenbo@public.cc.jl.cn (E. Wang).

0022-4596/$ - see front matter Crown Copyright © 2008 Published by Elsevier Inc. All rights reserved.
doi:10.1016/j.jssc.2008.10.039

Furthermore, the room temperature photoluminescence (PL) spectra of ZnO obtained in presence and absence of HPW were investigated, indicating that HPW affected on optical properties.

2. Experimental section

2.1. Materials

HPW was prepared according to the literature [25]. Zinc acetate dihydrate and ethanol purchased from Beijing Chemicals Co. Ltd. are of analytical grade and used as received without further purification.

2.2. Synthesis of ZnO hollow spheres

Zinc acetate dihydrate of 0.5 g was added into 15–20 mL of 1.0×10^{-3} mol/L HPW ethanol solution under magnetic stirring. After stirring for a few minutes, the mixture was transferred into a 23 mL Teflon-lined stainless autoclave. The autoclave was maintained at 120 °C for 48 h and then cooled to room temperature naturally. The obtained white precipitates were separated, washed with distilled water and ethanol and then dried at 60 °C for 8 h.

2.3. Characterization

The as-prepared samples were characterized by X-ray power diffraction (XRD) using a Rigaku D/max-IIB X-ray diffractometer with Cu$K\alpha$ ($\lambda = 1.5418$ Å) radiation in a 2θ range from 10° to 90° at room temperature. The microstructure of as-prepared samples were observed by transmission electron microscopy (TEM) and the selected area electron diffraction (SAED) using Hitachi-7500 electron microscopes at an accelerating voltage of 120 kV and by scanning electron microscopy (SEM) using JEOL JSM-840 electron microscope at an accelerating voltage of 20 kV. UV–vis absorption spectra were recorded using a 752 PC UV–vis spectrophotometer. The Fourier transform infrared (FTIR) absorption spectrum was obtained in the absorbance mode using a Bio-Rad FTS135 spectrophotometer. Nitrogen (N_2) adsorption–desorption isotherms were measured at liquid nitrogen temperature (77 K) using a NOVA l000 analyzer. The sample was degassed for 6 h at 150 °C before the measurements. Surface areas were calculated by the Brunauer–Emmett–Teller (BET) method from the data in the P/P_0 region 0.05–0.35 and pore sizes by the Barrett–Joyner–Halenda (BJH) method at a relative pressure of 0.95 (P/P_0). The room-temperature PL spectrum of the ZnO hollow spheres was performed on a JY-Labram spectrophotometer with a He–Cd laser as the excitation source at 325 nm.

3. Results and discussion

3.1. Characterization of ZnO hollow spheres

POM-controlled crystallization of ZnO crystals was performed under solvothermal condition. Fig. 1 shows the typical XRD pattern of as-prepared ZnO hollow spheres in the presence of HPW. All of the diffraction peaks can be perfectly indexed as hexagonal ZnO with lattice constants of $a = 3.249$ Å and $c = 5.206$ Å (JCPDS No. 36-1451). No diffraction peaks of other impurities are detected.

Low-magnification SEM image (Fig. 2a) shows the overall morphology of the ZnO hollow spheres prepared in the presence of HPW, indicating that as-prepared ZnO consists of nearly uniform spheres with diameters ranging from 400 to 600 nm

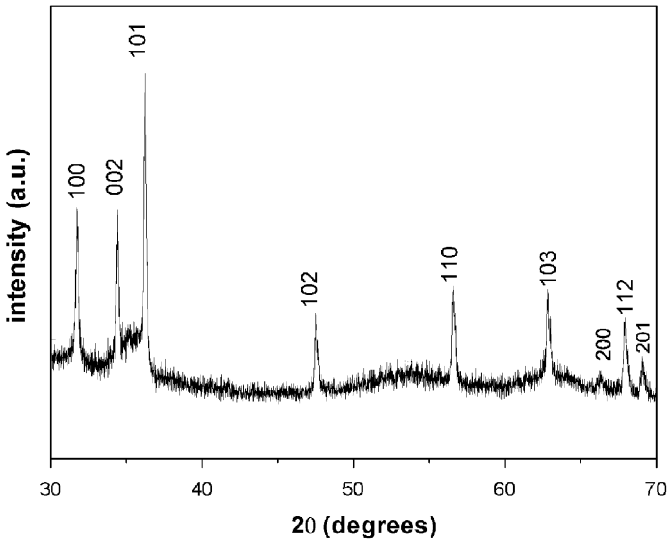

Fig. 1. Typical XRD pattern of ZnO hollow spheres.

and the thickness of shell was approximate 80 nm. High-magnification SEM image (Fig. 2b) shows that the outer surface of the hollow spheres was rough and stacked with small nanoparticles standing out of the surface. Furthermore, irregular pores could be observed on the surface of those spheres. Fig. 2c displays the SEM image of a cracked sphere with apparent cavity, demonstrating the hollow nature of the as-prepared ZnO spheres. It can be also found that the inner surface of the hollow sphere was also coarse and consisted of small nanoparticles with an average diameter of about 40 nm. It is worth noting that the hollow sphere is built from a single shell of small nanoparticles without any substrate support.

The morphology and structure of the ZnO hollow spheres were further studied with TEM and SAED. Fig. 2d shows typical TEM image of the as-prepared ZnO hollow spheres in the presence of HPW. The hollow nature of the spheres was also observed in the strong contrast between the dark edge and pale center, supporting the fact that the ZnO spheres have a hollow interior. The thickness of shells exhibits approximate 80 nm, in accord with the result of SEM (Fig. 2c). The SAED pattern in Fig. 2d (inset) shows that the hollow spheres behave as a polycrystalline phase.

The gas adsorption–desorption method was also employed to confirm the porosity of ZnO hollow spheres. Fig. 3a depicts the N_2 adsorption–desorption isotherm of the ZnO hollow spheres, indicating the existence of pores on the shell of the ZnO hollow spheres. The isotherm can be categorized as type IV, with a distinct hysteresis loop observed in the P/P_0 range of 0.55–0.95. The BET surface area is as high as 176.10 m^2/g calculated from the data in the P/P_0 region of 0.05–0.35. Fig. 3b shows the BJH pore-size distribution curve of ZnO hollow spheres, exhibiting pore size focusing in the range of 2–5 nm. These pores should originate from the interstices among the small spheric nanoparticles [26], in agreement with the SEM observations of hollow ZnO spheres (Fig. 2b and c).

3.2. Effect of reaction time on growth of ZnO hollow spheres

In order to clarify the morphology evolution of the ZnO hollow spheres, time-dependent experiments were performed in the presence of HPW without changing other experimental parameters. Typical TEM images of the products prepared at certain reaction time intervals shown in Fig. 4 demonstrate roughly a time-dependent deposition-dissolution process. When the

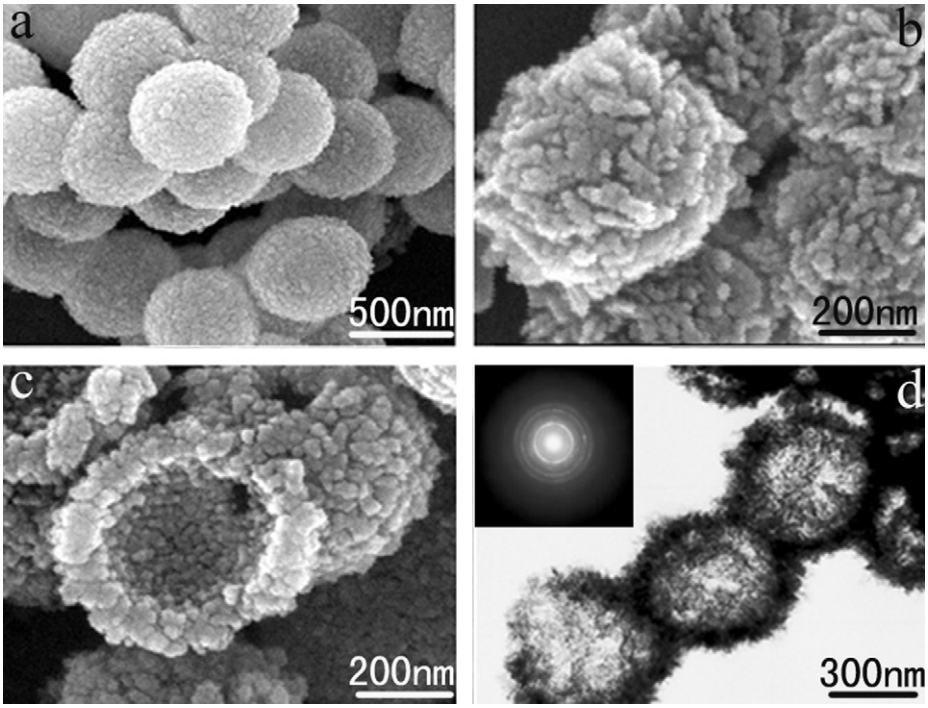

Fig. 2. Low-magnification (a) and high-magnification (b) SEM images of ZnO hollow spheres; (c) SEM image of a cracked sphere; and (d) TEM image of ZnO hollow spheres (the inset is its SAED).

reaction time was 1 h, irregular nanoparticles were obtained (Fig. 4a). When the reaction time was increased to 4 h, a small amount of solid spheres and relatively small nanoparticles coexisted (Fig. 4b). When the reaction time was prolonged to 12 h, perfect solid spheres were observed (Fig. 4c). A mixture of solid and hollow spheres was formed with the elongation of the time to 24 h (Fig. 4d). Interestingly, further increase of the reaction time for 36 h led to the formation of complete hollow spheres (Fig. 4e and f), which exhibited thicker shells than the hollow spheres prepared for 48 h as shown in Fig. 2d. Evidently, it is believed that the growth of the ZnO hollow spheres may be an oriented aggregation and dissolution process and the thickness of their shells was decreased with the increase of the reaction time. Namely, the reaction time plays an important role in controlling the formation of the ZnO hollow spheres.

3.3. Effect of reaction temperature on growth of ZnO hollow spheres

Controlled experiments were conducted in presence of HPW at different temperature without changing other reaction conditions and the resultant products were analyzed by TEM investigation. By solvothermal treatment at 100 °C, the product consisted of solid spheres and nanoparticles were obtained (Fig. 5a). Upon increasing the solvothermal temperature to 120 °C, product composed of perfect hollow spheres was obtained (Fig. 2). The hollow spheres obtained at 140 °C show thin and smooth shells (Fig. 5b) different from the product prepared at 120 °C (Fig. 2d). The experimental results indicate that a higher temperature and pressure is in favor of hollow cavity and the solvothermal temperature also plays an important role in controlling the formation of the ZnO hollow spheres.

3.4. Effect of HPW on growth of ZnO hollow spheres

Further controlled experiments indicated that HPW concentration played a key role in the formation of the ZnO hollow spheres. Fig. 5c shows typical TEM image of the sample obtained without HPW, indicating that no hollow spheres were obtained while only irregular nanoparticles were observed. In our previous work [27], the sample obtained in presence of 4×10^{-4} mol/L HPW existed in the form of irregular microparticles. Upon increasing HPW concentration to 1.0×10^{-3} mol/L, perfect hollow spheres were obtained as shown in Fig. 2a–d. Upon further increasing of HPW concentration to 2.0×10^{-3} mol/L, only irregular nanowires were observed (Fig. 5d). From the above controlled experiments, we conclude that the appropriate amount of the HPW must be crucial for controlling morphology of the ZnO hollow spheres.

Fig. 6 shows UV–vis absorbance spectra of the filtrate before (a) and after (b) solvothermal treatment at 120 °C for 48 h in present of HPW. Two characteristic bands were observed at about 210 nm and relative 260 nm, which are attributed to the O–W charge transfer transition of POMs [17]. The result demonstrates that the original framework of HPW is not destroyed after solvothermal treatment, implying that the HPW may serve as a catalyst, which has been used in the esterification reaction between alcohol and acetic acid towards ester [28]. Additionally, gas chromatography (GC) analysis is used to identify the formation of Acetyl acetate in the filtrate after solvothermal treatment as shown in Fig. S1 (Supporting Information), which further confirms the possibility of HPW as a catalyst in the current experiment.

FTIR spectrum is an effective method to reveal the composition of the products. Fig. 7 shows FTIR spectrum of the as-prepared ZnO hollow spheres. Seven peaks were observed. The two peaks at 3400 and 1626 cm^{-1} are attributed to O–H stretching vibration and H–O–H bending vibration, which are assigned to small amount of H_2O existing in the ZnO hollow spheres. The peak at 445 is ascribed to Zn–O stretching vibration. The four peaks at 1085, 985, 807, and 717 cm^{-1} are, respectively, assigned to an inner P–O_a–W bond, an external W=O_c bond, W–O_b–W, and W–O_d–W bridges (where O_a is the oxygen in P–O tetrahedron, O_d is the terminal oxygen, O_b is the bridging oxygen of two octahedra sharing a corner, and O_c is the bridging oxygen of two octahedra

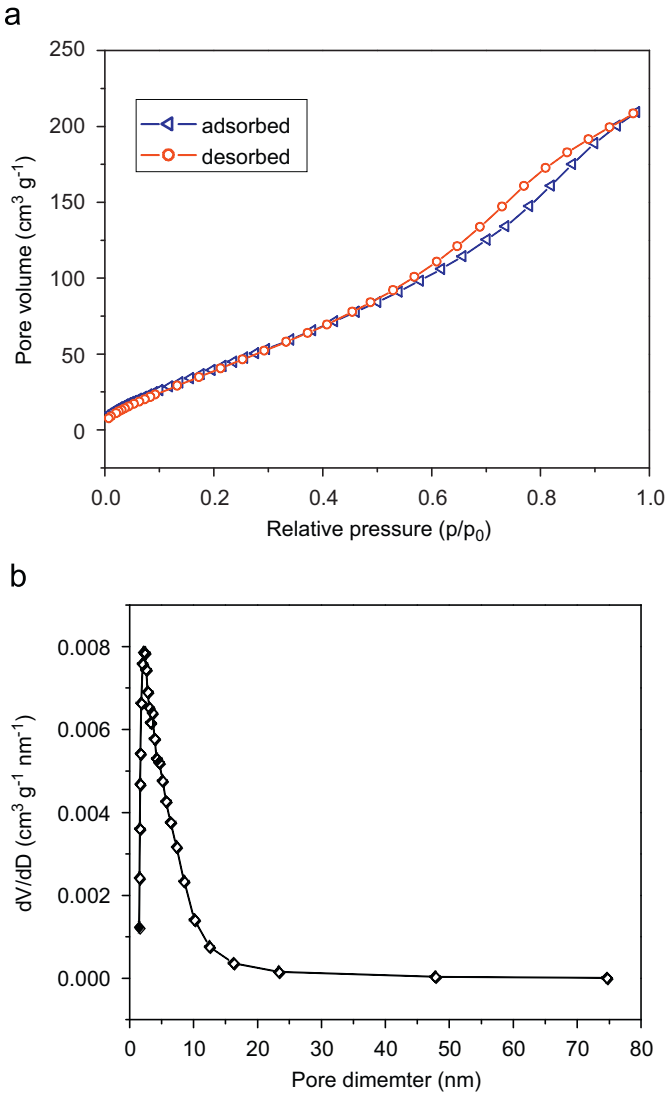

Fig. 3. Nitrogen adsorption–desorption isotherm (a) and BJH pore-size distribution curve (b) of ZnO hollow spheres.

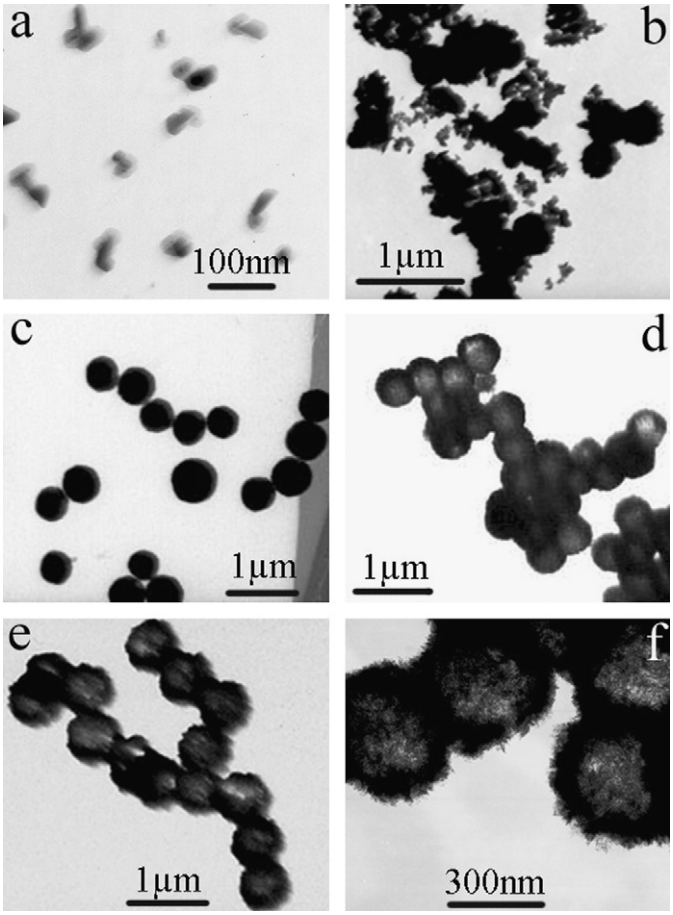

Fig. 4. TEM images of ZnO obtained with HPW at 120 °C for different time: (a) 1 h, (b) 4 h, (c) 12 h, (d) 24 h, (e) 36 h (low magnification) and (f) 36 h (high magnification).

sharing an edge) [17], indicating that there was HPW adsorbed on the surface of the ZnO hollow spheres. However, no diffraction peaks of HPW can be detected in XRD pattern (Fig. 1) of the ZnO hollow spheres, which may be due to very little HPW adsorbed on the surface of the ZnO hollow spheres.

3.5. Growth mechanism

In previous researches, the alcoholysis process of zinc acetate without HPW has been investigated and the formation of the synthesized ZnO nanoparticles is ascribed to the reaction between alcohol and acetate ion towards ester [29]. The chemical equations can be expressed as follows [29]:

$$CH_3COO^- + HO{-}CH_2CH_3 \rightarrow OH^- + CH_3COOCH_2CH_3 \quad (1)$$

$$Zn^{2+} + 2OH^- \rightarrow ZnO\downarrow + H_2O \quad (2)$$

The weak esterification (Eq. (1)) acted as OH^- reservoir and released OH^- gradually, and then Zn^{2+} cations reacted with OH^- anions to form ZnO nanoparticles (Eq. (2)) under solvothermal conditions [29]. As we know, POMs are one class of excellent catalysts owing to their unique electronic characteristics and structural robustness, especially as strong acid catalyst, which has been used in esterification reactions [17,28]. On the basis of the investigations described above, a possible growth mechanism of ZnO hollow spheres can be tentatively proposed in the current experimental conditions. From the kinetic point of view, the proposed formation process of ZnO hollow spheres could be divided into three steps as shown in Scheme 1. In the first steps, the catalysis action of HPW may accelerate the weak esterification (Eq. (1)), leading to releasing OH^- fleetly. As a result, massive ZnO nanoclusters were momentarily formed under mild solvothermal conditions (Eq. (2)). On the other hand, hexagonal ZnO crystal has a positively polar zinc face and a negatively polar oxygen face. Thus, negative charge PW released by HPW was adsorbed at the positive charge zinc face of ZnO through electrostatic action, resulting in temporary stabilization of ZnO nanoclusters [30]. In the second step, nascent ZnO nanoclusters preferentially aggregated and self-assembled into metastable spheres in order to minimize the total surface energy. The absorption of POMs on the surface of nanomaterials has been reported and employed for the morphology controlled syntheses of various nanomaterials [20–24]. In the final step, the metastable spheres were evolved into hollow spheres at the expense of interior small nanoclusters by a slow Ostwald ripening process [31–33]. Hollow interior structure obtained by this deposition–dissolution process is ascribed to the localized Ostwald ripening within metastable solid microspheres. Typically, this process is characterized by the initial deposition of amorphous microspheres and is likely to be highly sensitive to the relative rates of dissolution of the amorphous solid particles and nucleation of the crystalline phase.

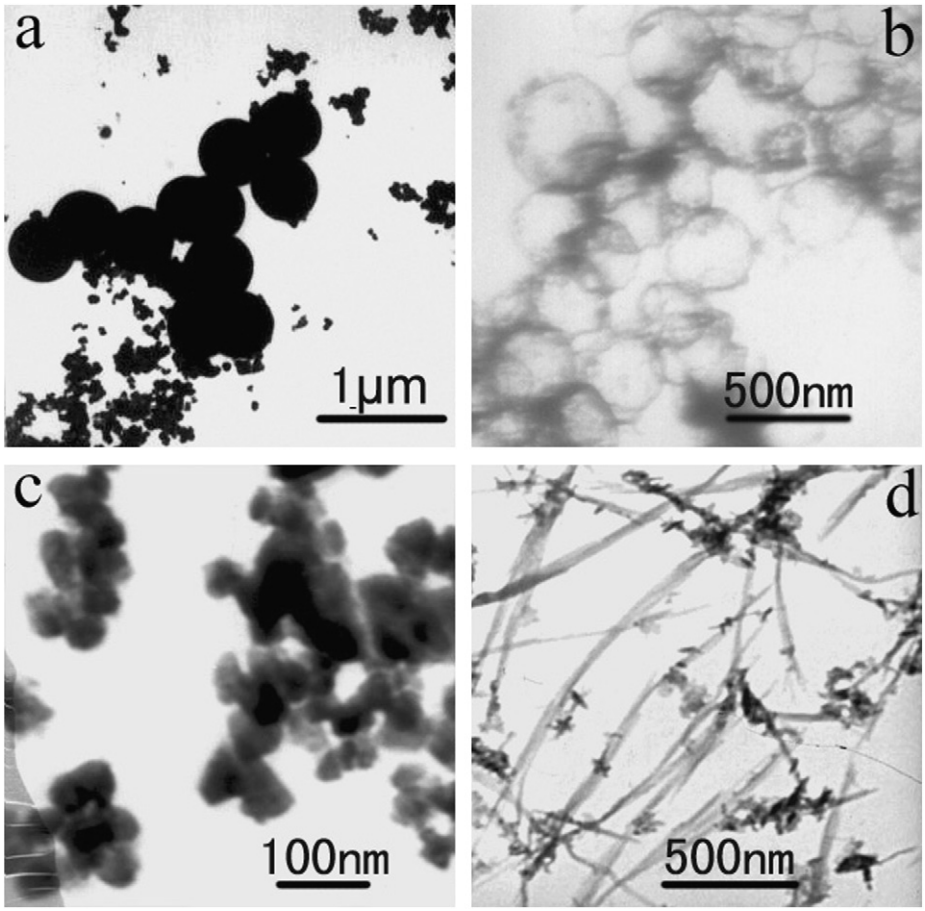

Fig. 5. TEM image of ZnO obtained for 48 h at different temperature: (a) 100 °C with 1.0×10^{-3} mol/L HPW, (b) 140 °C with 1.0×10^{-3} mol/L HPW, (c) 120 °C without HPW and (d) 120 °C with 2.0×10^{-3} mol/L HPW.

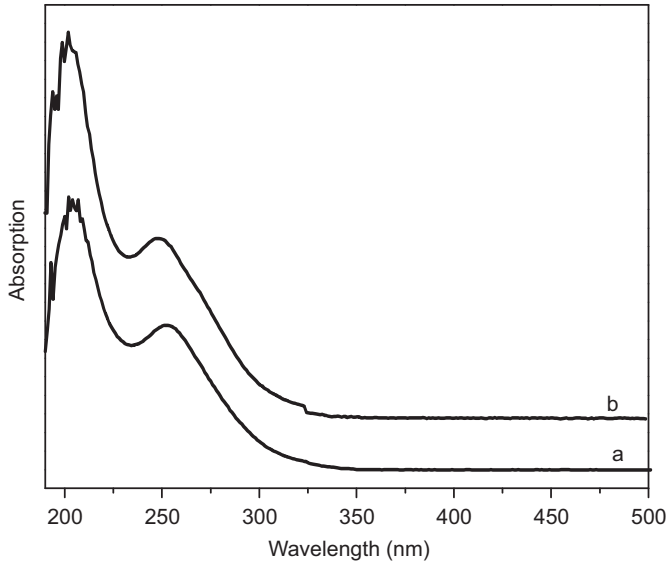

Fig. 6. UV–vis spectra of the filtrate before (a) and after (b) solvothermal treatment in present of HPW.

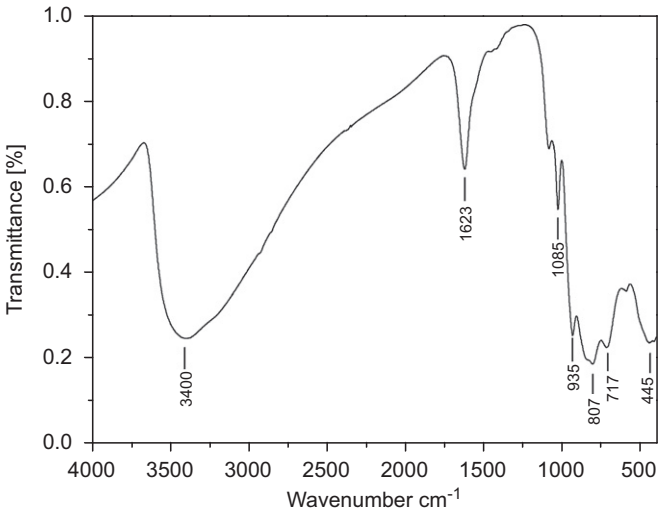

Fig. 7. FTIR spectrum of the ZnO hollow spheres.

In conclusion, the kinetic study illustrates that the formation of the hollow spheres is not a sudden sprouting process, but a slow developing one, which is supported by the time-dependent morphology evolution of the ZnO hollow spheres as shown in Fig. 4.

3.6. PL spectra

Fig. 8a displays the room temperature PL spectrum of the ZnO hollow spheres obtained in presence of HPW. One intense and broad yellow emission centered at about 555 nm in visible region was observed whereas a very weak ultraviolet emission at about 386 nm in ultraviolet region appeared. Generally, the ultraviolet

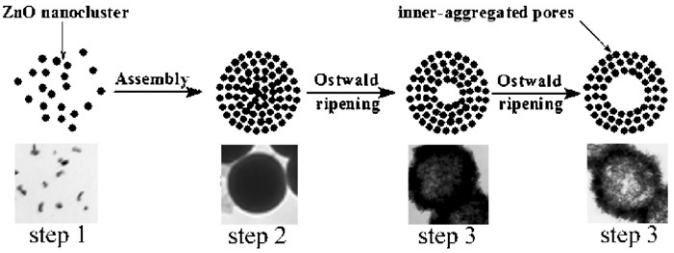

Scheme 1. The proposed formation process for ZnO hollow spheres.

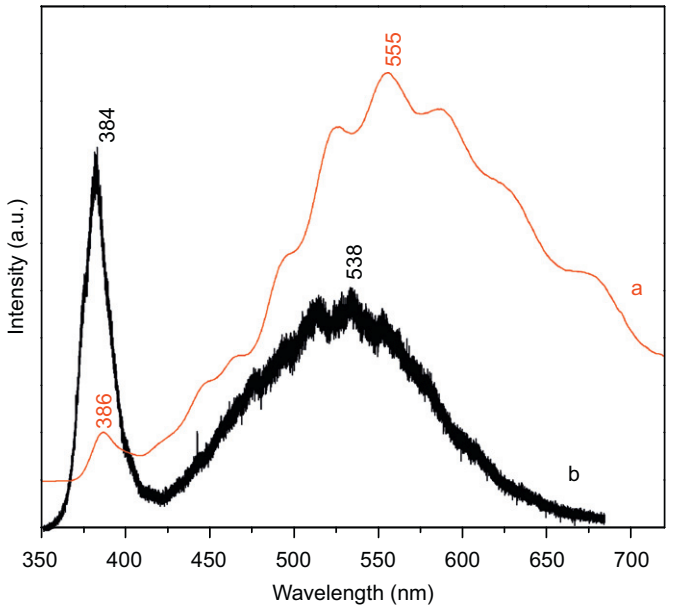

Fig. 8. Room temperature PL spectra of ZnO obtained in (a) presence and (b) absence of HPW.

emission is generated by the free-exciton recombination, whereas the visible emission is associated with defect-related transitions such as oxygen vacancies [34], zinc vacancies [35], zinc interstitials [36] and impurities [37]. Thus, the as-prepared ZnO hollow spheres possess abundant defects, which may be the reason that the hollow spheres are composed of much smaller ZnO nanoparticles with poor crystal.

To evaluate the effects of the HPW existing in the ZnO hollow spheres on PL properties, the room temperature PL spectrum of ZnO obtained without HPW was investigated as shown in Fig. 8b, indicating that a strong ultraviolet emission at about 384 nm and a weak broad green emission centered at about 538 nm, respectively. Compared to the two PL spectra, the visible emission enhanced and the UV emission quenched (Fig. 8a) may be due to the existence of HPW on the surface of ZnO hollow spheres besides their own intrinsic defects.

On the other hand, yellow and blue are complementary colors. When mixed together, yellow and blue lights can produce white light. Thus, the ZnO hollow spheres can be used as the coating layers of blue-light emitting diodes to produce white-light.

4. Conclusions

In summary, ZnO hollow spheres with porous shell were successfully synthesized by a one-pot solvothermal route in present of HPW without using any templates. HPW played a key role in the formation of the ZnO hollow spheres during the solvothermal treatment and the formation of the hollow spheres may be ascribed to a HPW-assisted assembly and slow Ostwald ripening dissolution process. This facile, low-cost and one-step process provides a rationally synthetic alternative for the preparation of ZnO hollow spheres with porous shell. Additionally, the room temperature PL spectrum of the ZnO hollow spheres exhibits a strong and broad yellow emission centered at around 555 nm in visible region. Thanks to the color complementarity of blue and yellow, the as-prepared ZnO hollow spheres may have potential applications in white-light emitting materials.

Acknowledgments

This work was financially supported by the National Natural Science Foundation of China (nos. 20701005/20701006); the Science and Technology Development Project Foundation of Jilin Province (no. 20060420); the Postdoctoral station Foundation of Ministry of Education (no. 20060200002); the Testing Foundation of Northeast Normal University; the Program for Changjiang Scholars and Innovative Research Team in University.

Appendix A. Supplementary material

Supplementary data associated with this article can be found in the online version at 10.1016/j.jssc.2008.10.039.

References

[1] F. Caruso, R.A. Caruso, H. Möhwald, Science 282 (1998) 1111–1114.
[2] Z. Zhong, Y. Yin, B. Gates, Y. Xia, Adv. Mater. 12 (2000) 206–209.
[3] F. Caruso, Adv. Mater. 13 (2001) 11–22.
[4] Z. Yang, Z. Niu, Y. Lu, Z. Hu, C.C. Han, Angew. Chem. Int. Ed. Engl. 42 (2003) 1943–1945.
[5] Y.G. Sun, Y.N. Xia, Science 298 (2002) 2176–2179.
[6] Y.L. Wang, L. Cai, Y.N. Xia, Adv. Mater. 17 (2005) 473–477.
[7] B.T. Holland, C.F. Blanford, A. Stein, Science 281 (1998) 538–540.
[8] A. Imhof, D.J. Pine, Nature 389 (1997) 948–951.
[9] M. Agrawal, A. Pich, N.E. Zafeiropoulos, S. Gupta, J. Pionteck, F. Simon, M. Stamm, Chem. Mater. 19 (2007) 1845–1852.
[10] M.C. Neves, T. Trindade, A.M.B. Timmons, J.D. Pedrosa de Jesus, Mater. Res. Bull. 36 (2001) 1099–1118.
[11] X. Wang, P. Hu, Y. Fangli, L. Yu, J. Phys. Chem. C 111 (2007) 6706–6712.
[12] H. Zhou, T.X. Fan, D. Zhang, Microporous Mesoporous Mater. 100 (2007) 322–327.
[13] B. Liu, H.C. Zeng, J. Am. Chem. Soc. 126 (2004) 16744–16746.
[14] M. Mo, J.C. Yu, L. Zhang, S.K.A. Li, Adv. Mater. 17 (2005) 756–760.
[15] S.Y. Gao, H.J. Zhang, X.M. Wang, R.P. Deng, D.H. Sun, G.L. Zhen g, J. Phys. Chem. B 110 (2006) 15847–15852.
[16] B. Liu, H.C. Zeng, Chem. Mater. 19 (2007) 5824–5826.
[17] M.T. Pope, A. Müller, Polyoxometalate Chemistry, Netherlands, 2001.
[18] J. Kim, L. Lee, B.K. Niece, J.X. Wang, A.A. Gewirth, J. Phys. Chem. B 108 (2004) 7927–7933.
[19] P. Garrigue, M.H. Delville, C. Labruge're, E. Cloutet, P.J. Kulesza, J.P. Morand, A. Kuhn, Chem. Mater. 16 (2004) 2984–2986.
[20] P.J. Kulesza, M. Chojak, K. Karnicka, K. Miecznikowski, B. Palys, A. Lewera, A. Wieckowski, Chem. Mater. 16 (2004) 4128–4134.
[21] Z.H. Kang, C.H.A. Tsang, Z.D. Zhang, M.L. Zhang, N.B. Wong, J.A. Zapien, Y.Y. Shan, S.T. Lee, J. Am. Chem. Soc. 129 (2007) 5326–5327.
[22] Z.H. Kang, E.B. Wang, B.D. Mao, Z.M. Su, L. Gao, S.Y. Lian, L. Xu, J. Am. Chem. Soc. 127 (2005) 6534–6535.
[23] B.D. Mao, Z.H. Kang, E.B. Wang, C.G. Tian, Z.M. Zhang, C.L. Wang, Y.L. Song, M.Y. Li, J. Solid State Chem. 180 (2007) 489–495.
[24] B.D. Mao, Z.H. Kang, E.B. Wang, C.G. Tian, Z.M. Zhang, C.L. Wang, S.H. Li, Chem. Lett. 36 (2007) 2–3.
[25] J.C. Bailar, Inorganic Synthesis, New York, 1939.
[26] Q.F. Zhang, T.P. Chou, B. Russo, S.A. Jenekhe, G.Z. Cao, Angew. Chem. Int. Ed. 47 (2008) 2402–2406.
[27] Q.Y. Li, Z.H. Kang, B.D. Mao, E.B. Wang, C.L. Wang, C.G. Tian, S.H. Li, Mater. Lett. 62 (2008) 2531–2534.
[28] E.B. Wang, Y.B. Tuan, Y.F. Zhang, Y.X. Zhou, Chinese J. Catal. 14 (1993) 147–149.
[29] H.C. Du, F.L. Yuan, S.L. Huang, J.L. Li, Y.F. Zhu, Chem. Lett. 33 (2004) 770–771.
[30] X. Wang, C.J. Summers, Z.L. Wang, Nano Letters 4 (2004) 423–426.

[31] H.G. Yang, H.C. Zeng, J. Phys. Chem. B. 108 (2004) 3492–3495.
[32] M.S. Mo, S.H. Lim, Y.W. Mai, R.K. Zheng, S.P. Ringer, Adv. Mater. 20 (2008) 339–342.
[33] J.G. Yu, H.T. Guo, S.A. Davis, S. Mann, Adv. Fun Mater. 16 (2006) 2035–2041.
[34] K.V. Vanheusden, W.L. Warren, C.H. Seager, J. Appl. Phys. 79 (1996) 7983–7990.
[35] Y.W. Heo, D.P. Norton, S.J. Pearton, J. Appl. Phys. 98 (2005) 0735021–0735026.
[36] X. Liu, X. Wu, H. Cao, R.P.H. Chang, J. Appl. Phys. 95 (2004) 3141–3147.
[37] N.Y. Garces, L. Wang, L. Bai, N.C. Giles, L.E. Halliburton, G. Antwell, Appl. Phys. Lett. 81 (2002) 622–624.